nanomaterials

MDPI

Article

Graphite Felt Modified by Atomic Layer Deposition with TiO_2 Nanocoating Exhibits Super-Hydrophilicity, Low Charge-Transform Resistance, and High Electrochemical Activity

Wen-Jen Lee [1,*], Yu-Ting Wu [1], Yi-Wei Liao [2] and Yen-Ting Liu [2]

[1] Department of Applied Physics, National Pingtung University, Pingtung 90003, Taiwan; sagessetim@gmail.com

[2] Department of Applied Chemistry, National Pingtung University, Pingtung 90003, Taiwan; aleweichart@gmail.com (Y.-W.L.); vancleefezz@gmail.com (Y.-T.L.)

* Correspondence: wenjenlee@mail.nptu.edu.tw; Tel.: +886-8-7663800

Received: 6 August 2020; Accepted: 28 August 2020; Published: 29 August 2020

Abstract: Graphite felt (GF) is a multi-functional material and is widely used as electrodes of electrochemical devices for energy and environmental applications. However, due to the inherent hydrophobicity of graphite felt, it must be hydrophilically pretreated to obtain good electrochemical activity. Metal oxides coating is one of the feasible methods to modify the surface of GF, and in order to ensure that the metal oxides have a better conductivity for obtaining higher electrochemical activity, a subsequent H_2 heat-treatment process is usually adopted. In this study, atomic layer deposition (ALD) is used to deposit TiO_2 nanocoating on graphite felt (GF) for surface modification without any H_2 thermal post-treatment. The results show that the ALD-TiO_2-modified GF (ALD-TiO_2/GF) owns excellent hydrophilicity. Moreover, the ALD-TiO_2/GF exhibits excellent electrochemical properties of low equivalent series resistance (R_s), low charge-transfer resistance (R_{ct}), and high electrochemical activity. It demonstrates that ALD is an applicable technique for modifying the GF surface. In addition, it can be reasonably imagined that not only TiO_2 film can effectively modify the GF surface, but also other metal oxides grown by ALD with nanoscale-thickness can also obtain the same benefits. We anticipate this work to be a starting point for modifying GF surface by using ALD with metal oxides nanocoating.

Keywords: graphite; graphite felt; carbon felt; atomic layer deposition; titanium dioxide; surface modification; hydrophilicity; electrochemical activity

1. Introduction

Graphite felt (GF) has a three-dimensional (3D) porous structure with high specific surface area [1,2] and numerous outstanding properties such as excellent electrical conductivity, flexibility, corrosion resistance and electrochemical stability [3,4]. Therefore, it has been widely studied as electrodes for energy and environmental applications that include vanadium redox flow batteries (VRFBs) [5,6], super capacitors [7–10], microbial fuel cells (MFCs) [11,12], biofuel cells (BFCs) [13,14], electro-Fenton (EF) process [15–17] and so forth.

However, GF has a hydrophobic surface property in nature, resulting in its poor electrochemical activity in aqueous solution and a low performance of GF-based electrochemical devices [18]. In order to improve the electrochemical activity of GF, the hydrophobic surface of original GF should be modified to hydrophilic surface, moreover, the GF should be maintained native good electrical conductivity simultaneously.

Kozbial et al. reported [19] that the hydrophobicity of graphite surface is attributed to the adsorption of hydrophobic organic pollutants (i.e., hydrocarbons) in the atmospheric environment and the graphite surface can be hydrophilic if the adsorbed organic pollutants are removed. In addition, Le et al. indicated that attaching oxygen-containing functional groups to the surface of GF can effectively increase its hydrophilicity and electrochemical activity [18].

Several methods have been successfully applied to modify the GF surface at various conditions, including plasma treatment [20,21], chemical treatment [22–27], thermal treatment [28–32], nitrogenization treatment [33–35], carbon nanomaterials based modification [36–39], nanostructural metals [40–43] and metal oxides [44,45] decorating.

In general, an appropriate method for surface-modification of GF must include the following requirements. Firstly, the method should change the GF surface from hydrophobic to hydrophilic property to obtain a low interface resistance (low charge-transfer resistance, R_{ct}) between the modified GF-based electrode and electrolyte for fast charge-transfer reactions. Secondly, the modified GF should maintain primitive excellent conductivity of original GF to receive a low equivalent series resistance (R_s). To improve the electrochemical activity of GF, all of the above characteristics should be satisfied simultaneously. Finally, the modified GF must maintain long-term stability of hydrophilicity and excellent chemical stability to sustain corrosive electrolyte of electrochemical devices such as vanadium redox flow batteries (VRFBs), aluminum-ion batteries and so forth.

The GF modified with metal oxides decorating or coating exhibits long-term stable hydrophilicity and chemical stability. However, the conductivity of metal oxides is generally varied with the impurity and defect concentration in the oxides. If the metal oxides have poor conductivity, the conductivity of GF will decrease and result in its poor electrochemical activity. Therefore, in order to enhance the electrochemical activity of GF modified with metal oxides, typically a post-annealing process in a reducing atmosphere (containing H_2 gas) is necessary. Because the concentration of oxygen vacancies in the lattice of metal oxides will be increased during the H_2 thermal treatment process to form defect-rich non-stoichiometric metal oxides, a lower resistance of metal oxides for obtaining higher electrochemical activity is found [46,47].

In this work, a nanocoating TiO_2 film (about 10 nm) is grown on the GF surface by atomic layer deposition (ALD) for surface-modification of GF and without any H_2 thermal treatment process. TiO_2 is a native hydrophilic material with outstanding chemical stability. Thus, the hydrophobic surface of GF can be modified to hydrophilic by coating with TiO_2 films, and the TiO_2 surface-coating can withstand the corrosion of strong corrosive electrolyte when the TiO_2-modified GF is applied to electrochemical devices. ALD is an advanced technique for growing highly conformal thin films on the surfaces of three-dimensional complex-structures and nanostructures with atomic-level thickness control and excellent coating uniformity [48–50]. Moreover, conformal TiO_2 thin films with nanoscale-thickness have been successfully coated on carbon nanotube (CNT) fibers and graphite fibers by using ALD technique [51–53]. Therefore, a 10-nm-thick TiO_2 film can be uniformly coated on the GF surface by ALD technology with accurate control of film thickness at the nanoscale. We make the TiO_2 film with an ultra-thin thickness of 10 nm and a nanocrystalline structure, which not only confers hydrophilicity to GF but also ensures that the ALD-TiO_2-modified GF (ALD-TiO_2/GF) has a sufficiently low resistance for achieving excellent electrochemical activity (the reason and design concept will be explained later).

The results show that the ALD-TiO_2/GF has a super-hydrophilic property and retains a good conductivity, the same as the original GF (see Supplementary Video and Materials, Figure S1). The electrochemical measurements of cyclic voltammetry (CV) and electrochemical impedance spectroscopy (EIS) show that the electrochemical activity of GF is significantly improved by an order of magnitude of two via ALD-TiO_2 modification. Besides, both original GF and ALD-TiO_2/GF have a similar low equivalent series resistance (R_s), which is about 5.85 and 3.62 Ω for original GF and ALD-TiO_2/GF, respectively. However, ALD-TiO_2/GF has a charge-transfer resistance (R_{ct}) of about 0.28 Ω, which is 100 times lower than the original GF of about 24.88 Ω.

As the excellent electrochemical properties, it is expected that the ALD-TiO_2/GF electrode has potential applications in vanadium redox flow batteries (VRFB), aluminum-ion batteries, and other electrochemical energy-storage devices. Additionally, this work demonstrates that ALD technology is an applicable method for surface modification of GF. It is believed that not only TiO_2 films are effective in modifying GF surface but also other metal oxide films grown by ALD with nanoscale thickness can be applied for surface modification of GF.

2. Materials and Methods

2.1. Surface Modification of GF

For surface modification of GF, a low-pressure ALD system was used to coat a thin TiO_2 film on the surface of GF (the thickness of GF is about 2 mm). The process includes 3 steps, as follows:

(1) Removing the surface-adsorbed organic pollutants of GF: the original GF was introduced into the ALD reactor and then the GF was annealed at 500 °C for 2 h in the ALD reactor. The purpose of this step is to remove organic pollutants adsorbed on the surface of GF by thermal decomposition, to ensure that the GF has a clean and hydrophilic surface for ALD process.

(2) Ultra-thin amorphous TiO_2 film coated on the GF surface by ALD: a 10-nm-thick TiO_2 film was coated on the GF surface by ALD with 100 ALD-cycles at 60 °C for which the details of the ALD process were described in our previous works [54–56]. Briefly, $TiCl_4$ and H_2O were used as the precursors, Ar was used as the purge gas, and the growth rate is about 0.1 nm per cycle. In this step, an ultra-thin amorphous TiO_2 film is uniformly coated on all the surfaces of the GF to form ALD-TiO_2/GF sample.

(3) Nanocrystallization of TiO_2 film: TiO_2 grown at the low temperature of 60 °C has an amorphous structure. In order to improve the corrosion resistance and activity of TiO_2, a post-annealing process was performed at 500 °C for 2h in the ALD reactor to transform the TiO_2 surface coating from an amorphous into an anatase crystal structure.

Design Concept of This Study

The design concept of the above process is shown in Figure 1. The well-known Equation (1) shows the relationship between the resistance, resistivity, length, and area of a material.

$$R = \rho \frac{L}{A} \quad (1)$$

where R is the resistance of the material, ρ is the resistivity of the material, L is the transmission length of charges transfer in the material, and A is the cross-sectional area of material perpendicular to the current direction. According to the Equation (1), it can be known that if we reduce ρ, shorten L or increase A, then the R will be reduced.

In this work, ρ is the resistivity of TiO_2 film, L is the thickness of TiO_2 film, and A is the surface area of graphite felt for TiO_2 film deposition. Thus, reducing ρ and L of TiO_2 film are the developing directions that can be striven in this work. In this study, in order to reduce the resistance (R) of the TiO_2 coating on the GF surface, on the one hand, a nanoscale-thick (~10 nm) TiO_2 film was grown on the GF to shorten L. On the other hand, a two-step process (firstly growing an amorphous film at low temperature, and then raising the temperature to crystallize the film) was used to obtain a nanocrystalline TiO_2 film. It is noticed that my previous work [55] and other previous studies [51,52] have confirmed that nanocrystalline TiO_2 films can be obtained by the two-step process. Since the nanocrystalline TiO_2 film has a large amount of grain boundary defects, the resistivity (ρ) of the TiO_2 film can be effectively reduced. As described above, the TiO_2 film with an ultra-thin thickness of 10 nm and a nanocrystalline structure can succeed a low resistance.

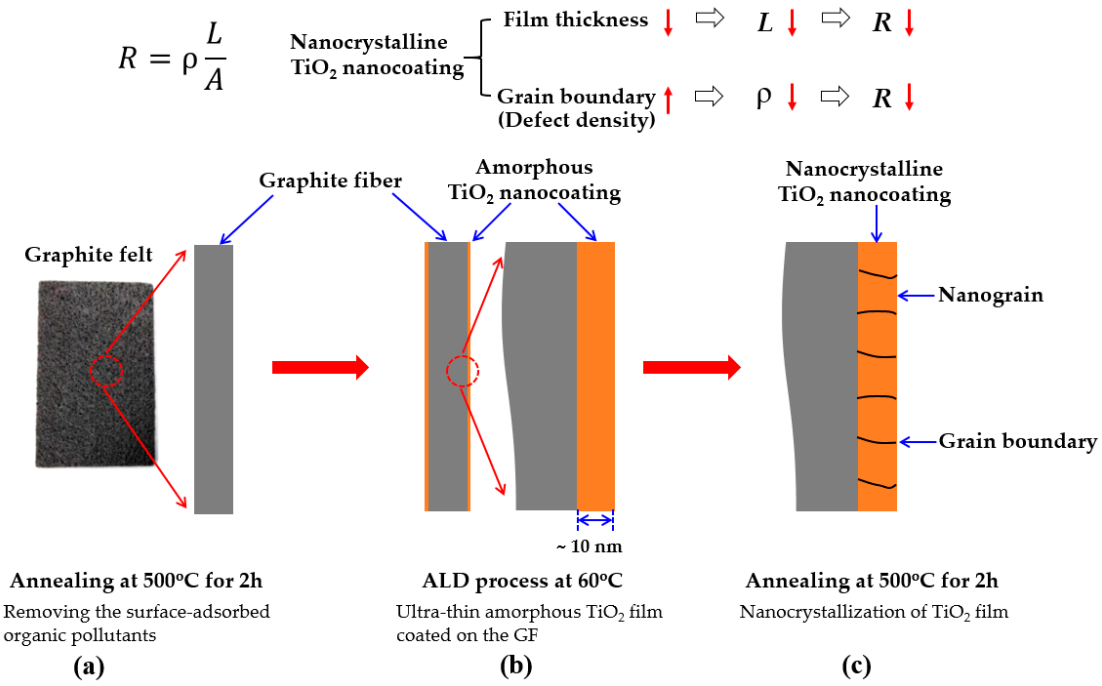

Figure 1. Schematic diagram of the design concept of this study. (**a**) Removing the surface-adsorbed organic pollutants of GF by thermal annealing process, (**b**) Ultra-thin amorphous TiO_2 film coated on the GF surface by ALD, and (**c**) Nanocrystallization of TiO_2 film by thermal annealing process.

2.2. Characterizations

Scanning electron microscopy (SEM) images and energy-dispersive X-ray spectroscopy (EDS) mapping analyses were carried out on a high-resolution scanning electron microscope (SU8000, Hitachi, Japan) provided with an energy-dispersive X-ray spectroscope (XFlash 5060FQ, Bruker, Germany). X-ray diffraction (XRD) patterns were performed on an X-ray diffractometer (D8 Advance Eco, Bruker, Germany). Raman spectra of the samples were examined by a micro Raman spectrometer (UniRAM II, Uninanotech, Korea).

2.3. Electrochemical Analysis

Figure 2 displays a schematic diagram of the electrochemical measurements. In order to enhance the difference between original GF and ALD-TiO_2-modified GF (ALD-TiO_2/GF), two pieces of original GFs or ALD-TiO_2/GFs with a length of 3 cm and a width of 1cm were used as electrodes and a 3M KCl aqueous solution was used as electrolyte, to configure two-electrode cells for electrochemical analyses. The electrochemical measurements of cyclic voltammetry (CV) and electrochemical impedance spectroscopy (EIS) were examined in the two-electrode cells by using a potentiostat (Autolab PGSTAT204, Metrohm AG, Switzerland). In addition, an electrochemistry software (Nova, Metrohm AG, Switzerland) was used to analyze the data of electrochemical measurements.

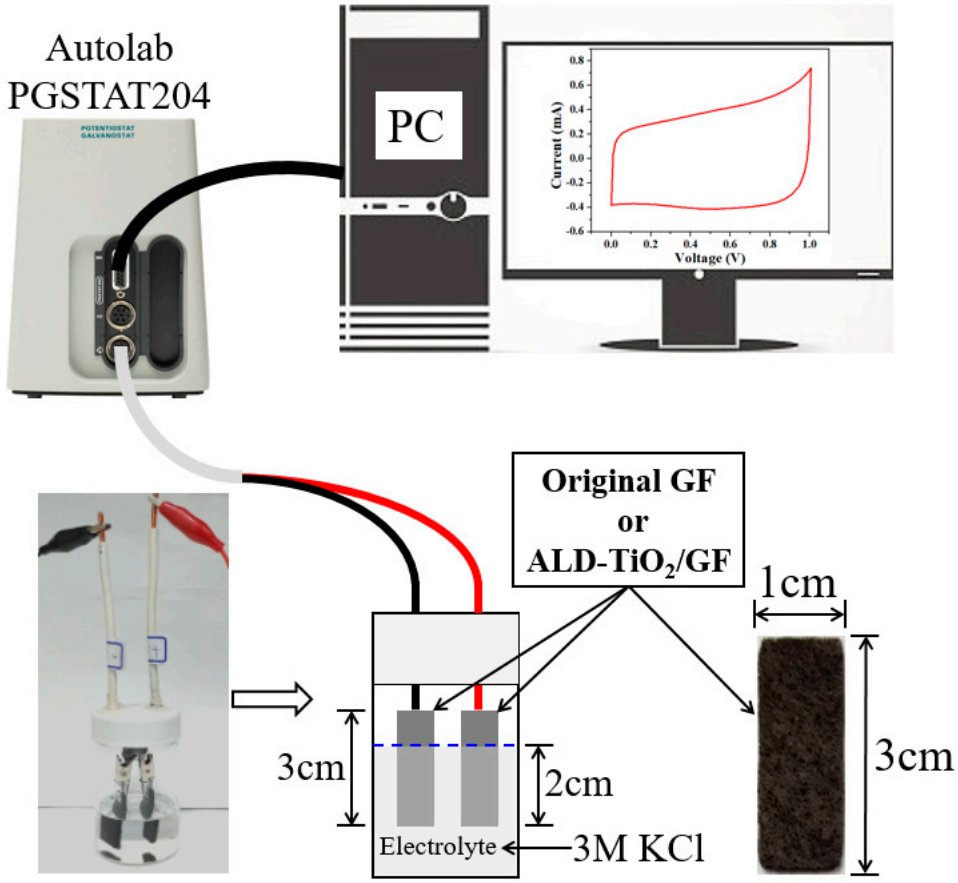

Figure 2. Schematic diagram of the electrochemical measurements.

3. Results and Discussion

The SEM images of original GF and ALD-TiO_2-modified GF (ALD-TiO_2/GF) are shown in the Figure 3. It is clearly showed that the GF is constructed from numerous carbon fibers with a diameter in the range of about 7–12 μm. Moreover, both original GF and ALD-TiO_2/GF have almost the same micromorphology (compare Figure 3a with Figure 3c) because the surface-coating of TiO_2 film is only 10 nm. However, the high-resolution images (Figure 3b,d) show that ALD-TiO_2/GF has a smoother surface than original GF and the surface nanopores of original GF are filled by ALD-TiO_2 coating. Figure 4 shows the elemental mapping images of selected-area EDS analysis for a carbon fiber of ALD-TiO_2/GF. It reveals that Ti and O atoms are distributed homogeneously on the carbon fiber, demonstrating that the thin TiO_2 film is coated uniformly on the GF by ALD.

Figure 5 shows the XRD patterns of original graphite felt (GF) and ALD-TiO_2-modified graphite felt (ALD-TiO_2/GF). Obviously, XRD peaks located at 2θ of 25.6, 43.6, 44.5 and 50.4° are observed in the XRD patterns that the XRD peaks of 25.6, 44.5 and 50.4° are corresponded to the (002), (101) and (102) planes of hexagonal Graphite-2H, and the XRD peaks of 25.6 and 43.6° can be indexed to the (003) and (101) planes of rhombohedral Graphite-3R, demonstrating that the crystal structure of GF is constructed from Graphite-2H with Graphite-3R. In addition, the XRD pattern of ALD-TiO_2/GF is almost the same as original GF and no XRD peak of TiO_2 crystal is detected because the thickness of TiO_2 surface coating is very thin (only about 10 nm), which is difficult to detect by XRD. Therefore, the samples are further analyzed by Raman spectrometer and the results are shown in the Figure 6.

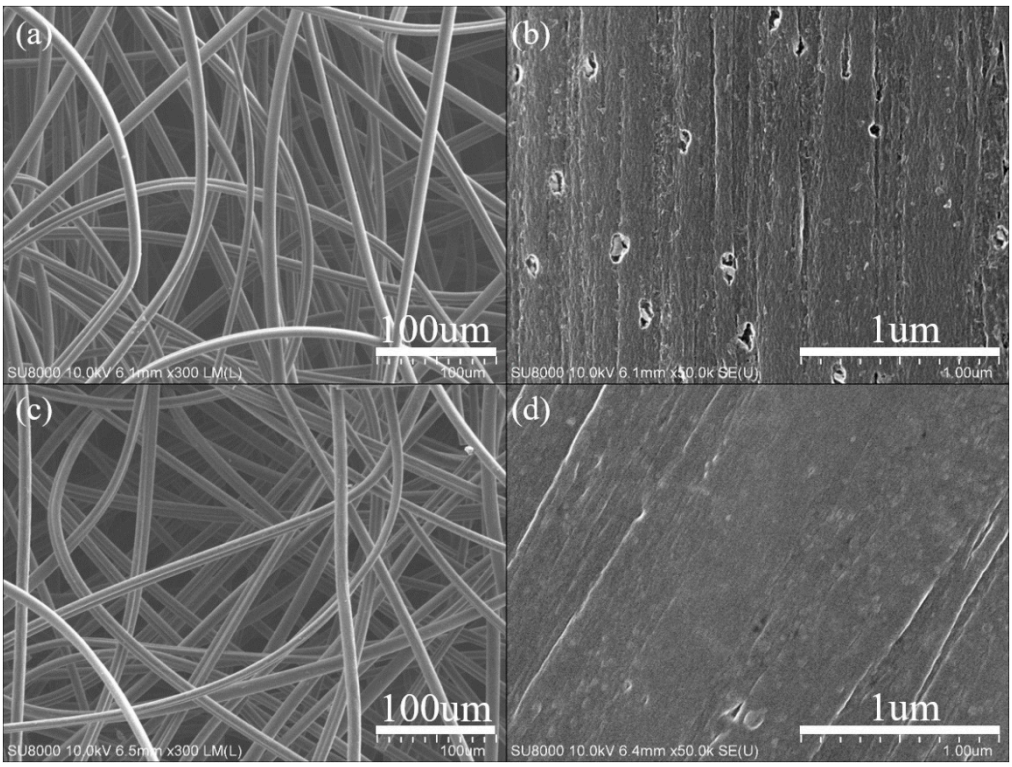

Figure 3. SEM images of original graphite felt (**a**,**b**) and atomic layer deposition (ALD)-TiO_2-modified graphite felt (**c**,**d**).

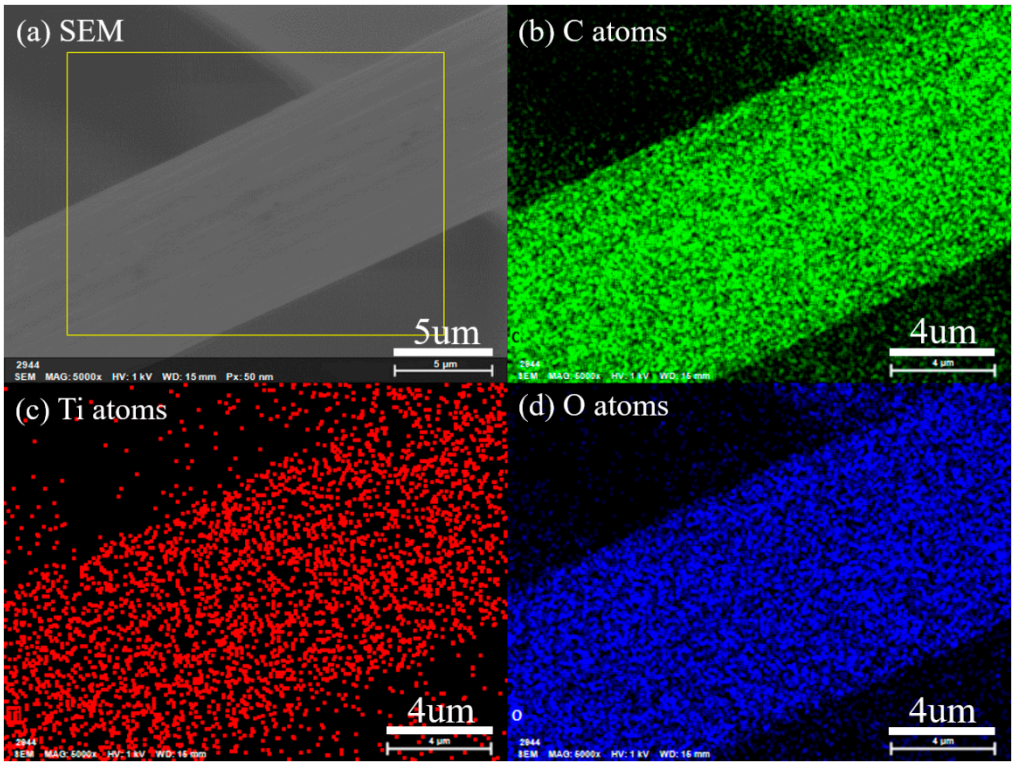

Figure 4. Energy-dispersive X-ray spectroscopy (EDS) mapping analysis of ALD-TiO_2-modified graphite felt. (**a**) SEM image of the selected-area EDS, and the elemental distribution images of (**b**) C, (**c**) Ti and (**d**) O atoms.

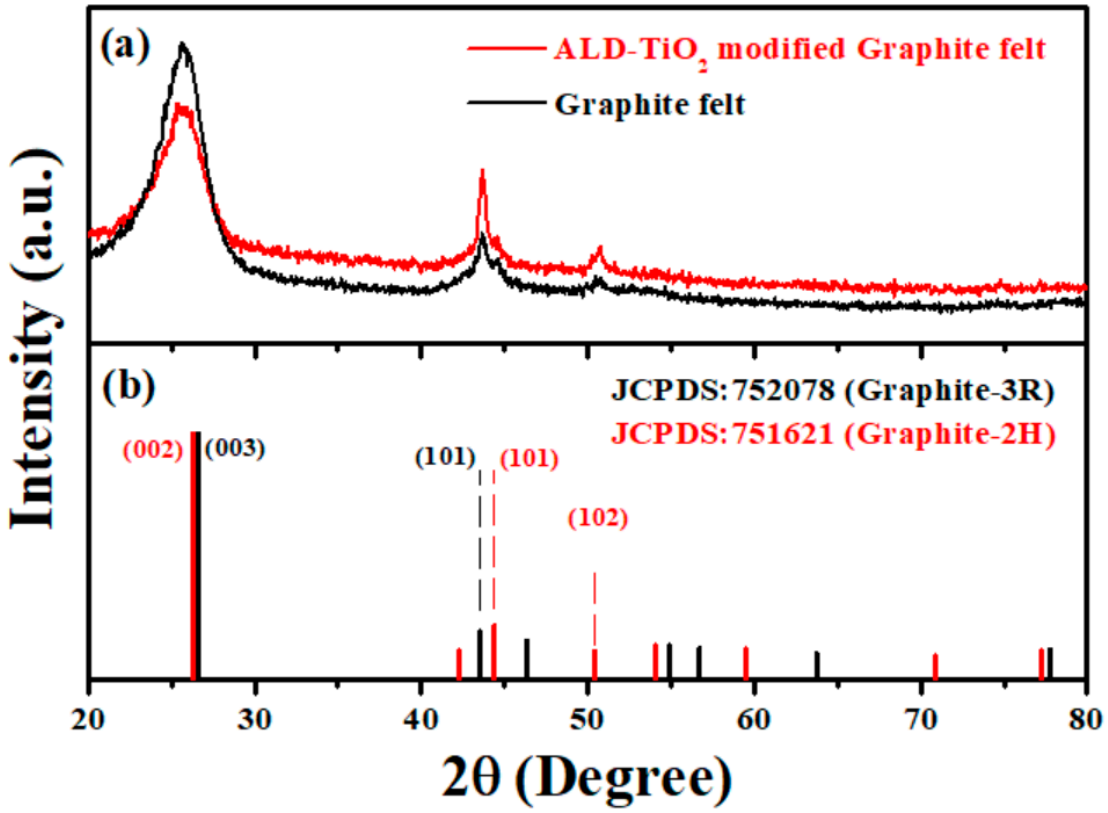

Figure 5. (**a**) XRD patterns of original graphite felt and ALD-TiO_2 modified graphite felt, (**b**) JPCDS cards of Graphite-3R and Graphite-2H.

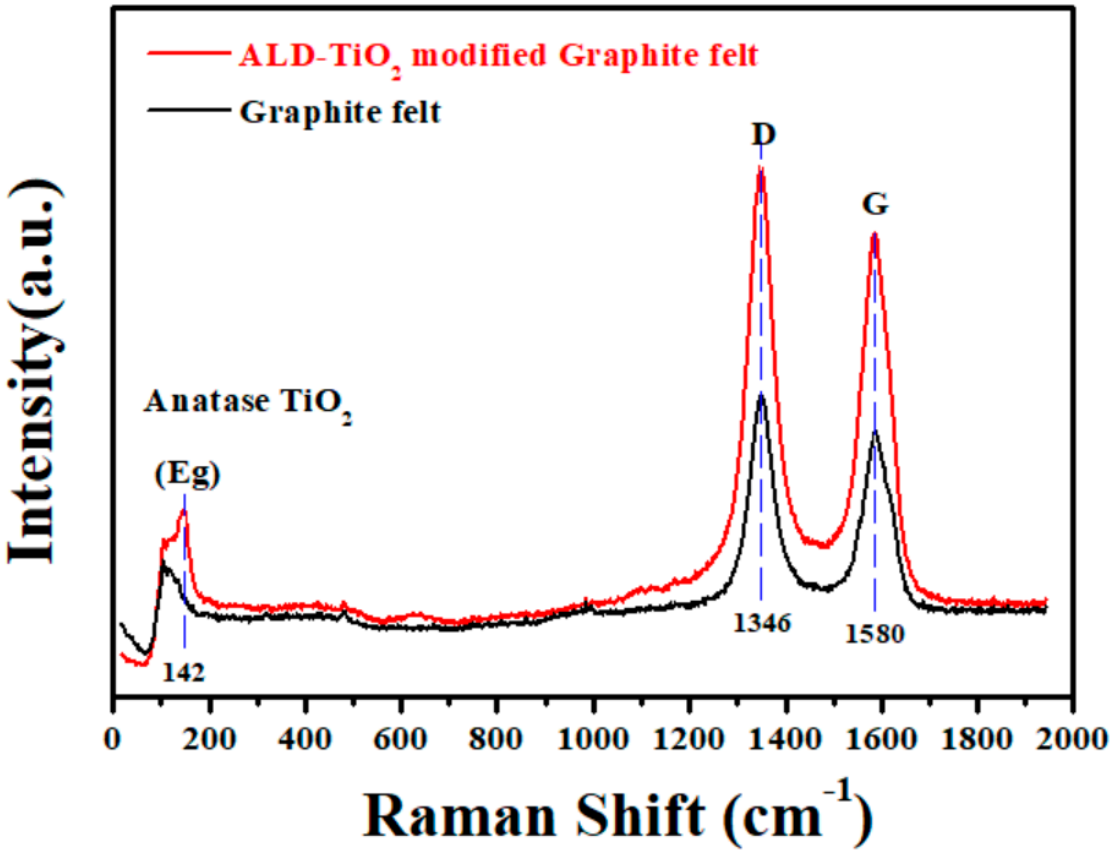

Figure 6. Raman spectra of original graphite felt and ALD-TiO_2-modified graphite felt.

In the Figure 6, two strong Raman peaks located at wavenumber 1346 and 1580 cm^{-1} are detected in the both original GF and ALD-TiO_2/GF. The Raman peaks of 1346 and 1580 cm^{-1} are indexed to the D-band (sp^3 carbon networks) and G-band (sp^2 carbon networks) of graphite, respectively [57,58]. In addition, a weak Raman peak located at around 142 cm^{-1} is also observed in the Raman spectrum of the ALD-TiO_2/GF, which can be indexed to the Eg mode of anatase TiO_2 [59–62], demonstrating that a thin anatase TiO_2 layer is coated on the GF surface.

In order to evaluate the electrochemical properties of original GF and ALD-TiO_2/GF, electrochemical measurements of cyclic voltammetry (CV) and electrochemical impedance spectroscopy (EIS) were performed. Figure 7a shows the CV curves of original GF and ALD-TiO_2/GF selected from the 10th cycle. Besides, the specific capacitances (calculated from CV measurements) of these electrodes as a function of cycle index are shown in Figure 7b. As shown in Figure 7a, the CV curve of ALD-TiO_2/GF exhibits quasi-rectangular shape and the area of CV curve of ALD-TiO_2/GF is significantly larger than the original GF. As shown in Figure 7b, the specific capacitances are about 0.16 and 23.65 mF/g on average for original GF and ALD-TiO_2/GF, respectively. It can be clearly seen that the electrochemical activity of GF is improved an order of magnitude of two. Besides, the ALD-TiO_2/GF has also demonstrated long-term stability, which is verified by a CV-test of 1000 cycles. The experimental data of 1000 times CV cycling-test are shown in the Supplementary Materials (Figure S2).

The enhancement of electrochemical activity of GF by ALD-TiO_2 surface modification can be reasonably attributed to the hydrophobic surface of GF which has been changed to super-hydrophilic, therefore, the equivalent series resistance (R_s) and charge-transfer resistance (R_{ct}) of between ALD-TiO_2/GF electrodes and electrolyte can be effectively reduced. In order to prove that the R_s and R_{ct} of ALD-TiO_2/GF electrodes are lower than original GF, the measurements of electrochemical impedance spectroscopy (EIS) were carried out. The EIS is a powerful tool, which has been widely used for analyzing the internal resistance of electrodes and the resistance between the electrode and electrolyte [63–65].

Figure 8 reveals the Nyquist plots of the original GF and ALD-TiO_2/GF performed by EIS measurement. The Figure 8 exhibits a clear evidence that the equivalent series resistance (R_s) and charge-transfer resistance (R_{ct}) of ALD-TiO_2/GF electrodes are lower than the original GF. The R_s and R_{ct} are about 5.85 and 24.88 Ω for the original GF (as Figure 8b) and are about 3.62 and 0.28 Ω for ALD-TiO_2/GF (as Figure 8c). Besides, it is noticed that both the original GF and ALD-TiO_2/GF have a similar R_s value. However, the R_{ct} value of ALD-TiO_2/GF is 100 times lower than that of the original GF, proving that the significant increase (100 times) in electrochemical activity is primarily due to the contribution of the decrease in the R_{ct} value between the electrode and the electrolyte.

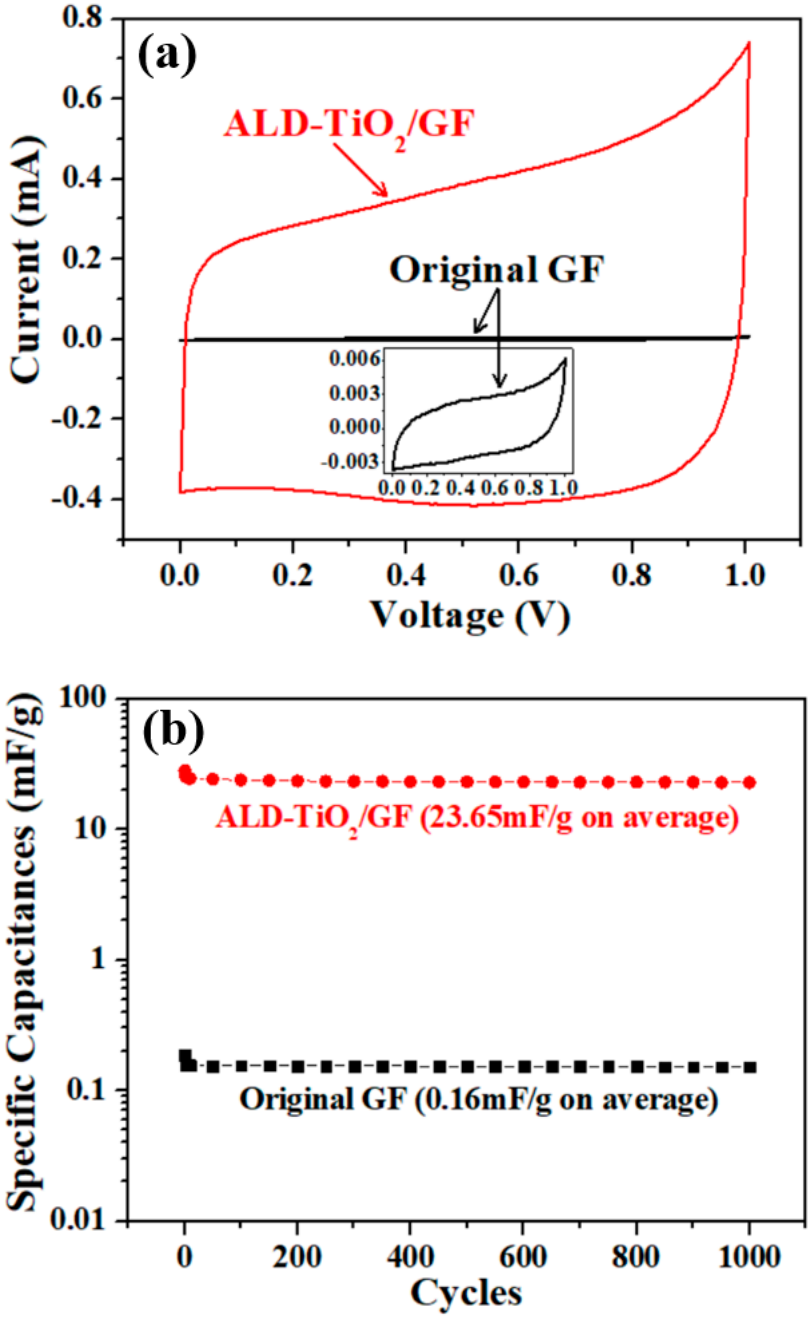

Figure 7. (**a**) Cyclic voltammetry (CV) curves of the original graphite felt (GF) and ALD-TiO_2 modified GF (ALD-TiO_2/GF), the scan rate is 1 V/s. (**b**) Specific capacitances of original GF and ALD-TiO_2/GF obtained from 1000 times CV cycling-test.

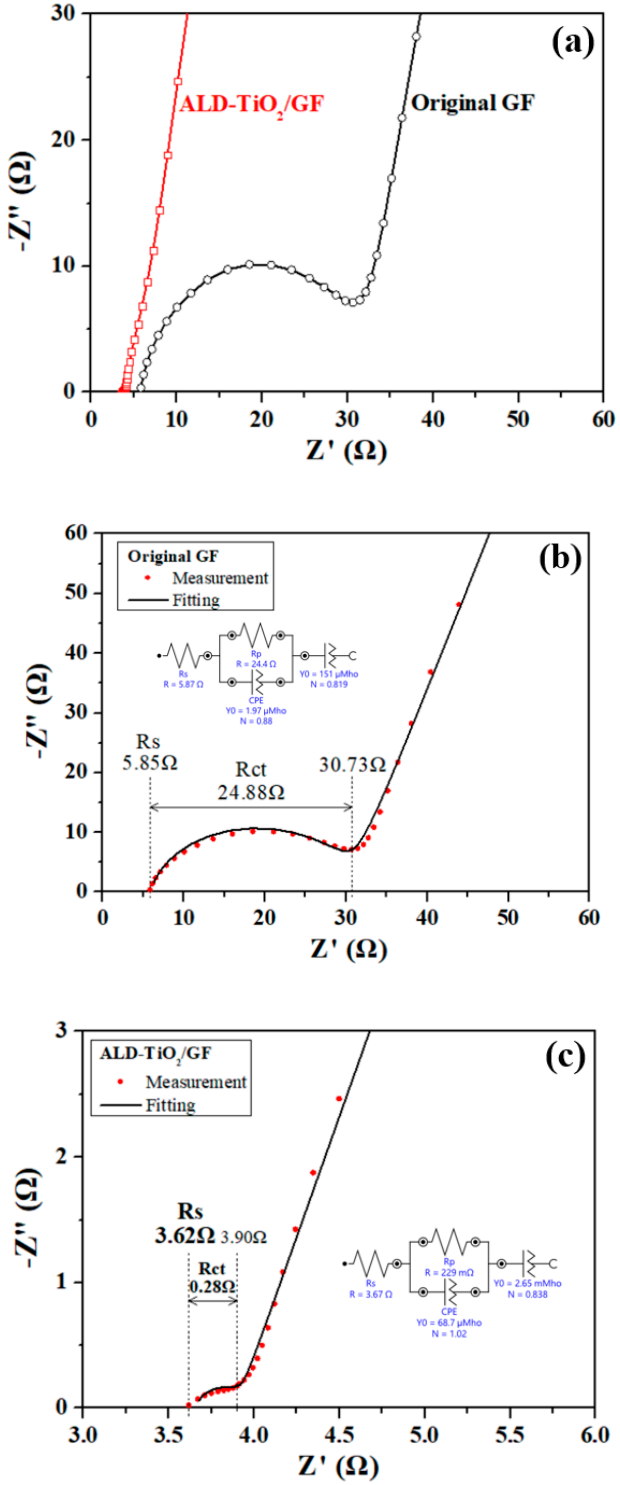

Figure 8. Nyquist plots of the original GF and ALD-TiO_2/GF measured by electrochemical impedance spectroscopy (EIS) measurement. (**a**) Compared figure of the original GF and ALD-TiO_2/GF, (**b**) and (**c**) show the experimental (red dots) and fitting (black line) data for the original GF and ALD-TiO_2/GF, respectively.

4. Conclusions

In conclusion, ALD technique with TiO_2 nanocoating is successfully employed as a new method for surface modification of GF to obtain excellent hydrophilicity, low equivalent series resistance (R_s), low charge-transfer resistance (R_{ct}), and high electrochemical activity. Especially, no any H_2 thermal

post-treatment is required. These excellent properties make ALD-TiO_2/GF have the potential to be used in electrochemical energy storage devices. We are currently conducting research and process optimization on applying ALD-TiO_2/GF to vanadium redox flow batteries (VRFBs). In addition, it can be reasonably anticipated that not only TiO_2 but also other metal oxides with nanoscale-thickness grown by ALD can be possibly applied to effectively modify the GF surface.

Supplementary Materials: A supplementary video and Supplementary Materials are available online at http://www.mdpi.com/2079-4991/10/9/1710/s1, The video demonstrates a simple-test of conductivity and hydrophilicity of original GF and ALD-TiO_2/GF. Figure S1: Simple-test for conductivity and hydrophilicity of original GF and ALD-TiO_2/GF. Figure S2: 1000 times CV cycling-test of original GF and ALD-TiO_2/GF.

Author Contributions: W.-J.L. conceived of the proposed idea, designed the experiments, verified the experimental data, and wrote the manuscript. Y.-T.W., Y.-W.L. and Y.-T.L. completed all the experimental works (including the supplementary video and materials) together and wrote part of the draft manuscript. Y.-T.W. is a master student Y.-W.L. and Y.-T.L. are undergraduate students, and W.-J.L. is their advising professor. All authors have read and agreed to the published version of the manuscript.

Funding: This research was funded by the Ministry of Science and Technology of Taiwan (No.: MOST 108-2622-E-153-001-CC3 and 108-2112-M-153-001).

Acknowledgments: The authors would like to thank Hui-Jung Shih (Instrument Center, NCKU) for assisting in HR-SEM and EDS analysis.

Conflicts of Interest: The authors declare no conflict of interest.

References

1. Shao, Y.; Cheng, Y.; Duan, W.; Wang, W.; Lin, Y.; Wang, Y.; Liu, J. Nanostructured electrocatalysts for PEM fuel cells and redox flow batteries: A selected review. *ACS Catal.* **2015**, *5*, 7288–7298. [CrossRef]
2. Zhang, Z.; Xi, J.; Zhou, H.; Qiu, X. KOH etched graphite felt with improved wettability and activity for vanadium flow batteries. *Electrochim. Acta* **2016**, *218*, 15–23. [CrossRef]
3. Wu, L.; Wang, J.; Shen, Y.; Liu, L.; Xi, J. Electrochemical evaluation methods of vanadium flow battery electrodes. *Phys. Chem. Chem. Phys.* **2017**, *19*, 14708–14717. [CrossRef] [PubMed]
4. Castañeda, L.F.; Walsh, F.C.; Nava, J.L.; León, C.P.D. Graphite felt as a versatile electrode material: Properties, reaction environment, performance and applications. *Electrochim. Acta* **2017**, *258*, 1115–1139. [CrossRef]
5. Kabtamu, D.M.; Chen, J.Y.; Chang, Y.C.; Wang, C.H. Water-activated graphite felt as a high-performance electrode for vanadium redox flow batteries. *J. Power Sources* **2017**, *341*, 270–279. [CrossRef]
6. Jianga, F.; Heb, Z.; Guoa, D.; Zhoua, X. Carbon aerogel modified graphite felt as advanced electrodes for vanadium redox flow batteries. *J. Power Sources* **2019**, *440*, 227114. [CrossRef]
7. Hea, M.; Zheng, Y.; Du, Q. Three-dimensional polypyrrole/MnO_2 composite networks deposited on graphite felt as free-standing electrode for supercapacitors. *Mater. Lett.* **2013**, *104*, 48–52. [CrossRef]
8. Díaz, P.; González, Z.; Santamaría, R.; Granda, M.; Menéndez, R.; Blanco, C. Enhanced energy density of carbon-based supercapacitors using cerium (III) sulphate as inorganic redox electrolyte. *Electrochim. Acta* **2015**, *168*, 277–284. [CrossRef]
9. Park, C.; Hwang, J.; Hwang, Y.T.; Song, C.; Ahn, S.; Kim, H.S.; Ahn, H. Intense pulsed white light assisted fabrication of Co-CoO_x core-shell nanoflakes on graphite felt for flexible hybrid supercapacitors. *Electrochim. Acta* **2017**, *246*, 757–765. [CrossRef]
10. Shen, P.; Wang, Z.; Yang, C.; Zhao, L.; Liu, T.; Shen, M.; Li, J.; Qian, D. Enhanced electrochemical property of graphite felt@$Co_2(OH)_2CO_3$ via Ni-P electrodeposition for flexible supercapacitors. *Electrochim. Acta* **2018**, *283*, 1568–1577. [CrossRef]
11. Pu, K.B.; Lu, C.X.; Zhang, K.; Zhang, H.; Chen, Q.Y.; Wang, Y.H. In situ synthesis of polypyrrole on graphite felt as bio-anode to enhance the start-up performance of microbial fuel cells. *Bioprocess Biosyst. Eng.* **2020**, *43*, 429–437. [CrossRef] [PubMed]
12. Liang, Y.; Zhai, H.; Liu, B.; Ji, M.; Li, J. Carbon nanomaterial-modified graphite felt as an anode enhanced the power production and polycyclic aromatic hydrocarbon removal in sediment microbial fuel cells. *Sci. Total Environ.* **2020**, *713*, 136483. [CrossRef] [PubMed]

13. Palmore, G.T.R.; Bertschy, H.; Bergens, S.H.; Whitesides, G.M. A methanol/dioxygen biofuel cell that uses NAD^+-dependent dehydrogenases as catalysts: Application of an electro-enzymatic method to regenerate nicotinamide adenine dinucleotide at low overpotentials. *J. Electroanal. Chem.* **1998**, *443*, 155–161. [CrossRef]
14. Séamus, F.D.; Higson, P.J. Biofuel cells—Recent advances and applications. *Biosens. Bioelectron.* **2007**, *22*, 1224–1235.
15. Liu, X.; Yang, D.; Zhou, Y.; Zhang, J.; Luo, L.; Meng, S.; Chen, S.; Tan, M.; Li, Z.; Tang, L. Electrocatalytic properties of N-doped graphite felt in electro-Fenton process and degradation mechanism of levofloxacin. *Chemosphere* **2017**, *182*, 306–315. [CrossRef]
16. Liang, L.; Yu, F.; An, Y.; Liu, M.; Zhou, M. Preparation of transition metal composite graphite felt cathode for efficient heterogeneous electro-Fenton process. *Environ. Sci. Pollut. Res.* **2017**, *24*, 1122–1132. [CrossRef]
17. Zhang, Y.; Zuo, S.; Zhou, M.; Liang, L.; Ren, G. Removal of tetracycline by coupling of flow-through electro-Fenton and in-situ regenerative active carbon felt adsorption. *Chem. Eng. J.* **2018**, *335*, 685–692. [CrossRef]
18. Le, T.X.; Bechelany, M.; Cretin, M. Carbon felt based-electrodes for energy and environmental applications: A review. *Carbon* **2017**, *122*, 564–591.
19. Kozbial, A.; Zhou, F.; Li, Z.; Liu, H.; Li, L. Are graphitic surfaces hydrophobic? *Acc. Chem. Res.* **2016**, *49*, 2765–2773. [CrossRef]
20. Chen, J.Z.; Liao, W.Y.; Hsieh, W.Y.; Hsu, C.C.; Chen, Y.S. All-vanadium redox flow batteries with graphite felt electrodes treated by atmospheric pressure plasma jets. *J. Power Sources* **2015**, *274*, 894–898. [CrossRef]
21. Dixon, D.; Babu, D.J.; Langner, J.; Bruns, M.; Pfaffmann, L.; Bhaskar, A. Effect of oxygen plasma treatment on the electrochemical performance of the rayon and polyacrylonitrile based carbon felt for the vanadium redox flow battery application. *J. Power Sources* **2016**, *332*, 240–248. [CrossRef]
22. Sun, B.; Skyllas-Kazacos, M. Chemical modification of graphite electrode materials for vanadium redox flow battery application-part II. Acid treatments. *Electrochim. Acta* **1992**, *37*, 2459–2465. [CrossRef]
23. Yue, L.; Li, W.; Sun, F.; Zhao, L.; Xing, L. Highly hydroxylated carbon fibres as electrode materials of all-vanadium redox flow battery. *Carbon* **2010**, *48*, 3079–3090. [CrossRef]
24. Flox, C.; Rubio-García, J.; Skoumal, M.; Andreu, T.; Morante, J.R. Thermo-chemical treatments based on NH_3/O_2 for improved graphite-based fiber electrodes in vanadium redox flow batteries. *Carbon* **2013**, *60*, 280–288. [CrossRef]
25. Ding, C.; Zhang, H.; Li, X.; Liu, T.; Xing, F. Vanadium flow battery for energy storage: Prospects and challenges. *J. Phys. Chem. Lett.* **2013**, *4*, 1281–1294. [CrossRef]
26. Di Blasi, A.; Briguglio, N.; Di Blasi, O.; Antonucci, V. Charge-discharge performance of carbon fiber-based electrodes in single cell and short stack for vanadium redox flow battery. *Appl. Energy* **2014**, *125*, 114–122. [CrossRef]
27. Hidalgo, D.; Tommasi, T.; Bocchini, S.; Chiolerio, A.; Chiodoni, A.; Mazzarino, I. Surface modification of commercial carbon felt used as anode for Microbial Fuel Cells. *Energy* **2016**, *99*, 193–201. [CrossRef]
28. Sun, B.; Skyllas-Kazacos, M. Modification of graphite electrode materials for vanadium redox flow battery application-I. Thermal treatment. *Electrochim. Acta* **1992**, *37*, 1253–1260. [CrossRef]
29. González, Z.; Botas, C.; Álvarez, P.; Roldán, S.; Blanco, C.; Santamaría, R.; Granda, M.; Menéndez, R. Thermally reduced graphite oxide as positive electrode in vanadium redox flow batteries. *Carbon* **2012**, *50*, 828–834. [CrossRef]
30. Pezeshki, A.M.; Clement, J.T.; Veith, G.M.; Zawodzinski, T.A.; Mench, M.M. High performance electrodes in vanadium redox flow batteries through oxygen-enriched thermal activation. *J. Power Sources* **2015**, *294*, 333–338. [CrossRef]
31. Le, T.X.H.; Charmette, C.; Bechelany, M.; Cretin, M. Facile preparation of porous carbon cathode to eliminate paracetamol in aqueous medium using electro-Fenton system. *Electrochim. Acta* **2016**, *188*, 378–384. [CrossRef]
32. Liu, T.; Li, X.; Xu, C.; Zhang, H. Activated carbon fiber paper based electrodes with high electrocatalytic activity for vanadium flow batteries with improved power density. *ACS Appl. Mater. Interfaces* **2017**, *9*, 4626–4633. [CrossRef]
33. Wang, P.; Lai, B.; Li, H.; Du, Z. Deposition of Fe on graphite felt by thermal decomposition of $Fe(CO)_5$ for effective cathodic preparation of microbial fuel cells. *Bioresour. Technol.* **2013**, *134*, 30–35. [CrossRef] [PubMed]

34. Chen, S.; Hu, W.; Hong, J.; Sandoe, S. Electrochemical disinfection of simulated ballast water on PbO_2/graphite felt electrode. *Mar. Pollut. Bull.* **2016**, *105*, 319–323. [CrossRef] [PubMed]
35. Zhang, C.; Liang, P.; Yang, X.; Jiang, Y.; Bian, Y.; Chen, C.; Zhanga, X.; Huanga, X. Binder-free graphene and manganese oxide coated carbon felt anode for high-performance microbial fuel cell. *Biosens. Bioelectron.* **2016**, *81*, 32–38. [CrossRef]
36. Mauricio Rosolen, J.; Patrick Poá, C.H.; Tronto, S.; Marchesin, M.S.; Silva, S.R.P. Electron field emission of carbon nanotubes on carbon felt. *Chem. Phys. Lett.* **2006**, *424*, 151–155. [CrossRef]
37. Rosolen, J.M.; Tronto, S.; Marchesin, M.S.; Almeida, E.C.; Ferreira, N.G.; Patrick Poa, C.H.; Ravi, S.; Silvad, P. Electron field emission from composite electrodes of carbon nanotubes-boron-doped diamond and carbon felts. *Appl. Phys. Lett.* **2006**, *88*, 083116. [CrossRef]
38. Wang, S.; Zhao, X.; Cochell, T.; Manthiram, A. Nitrogen-doped carbon nanotube/graphite felts as advanced electrode materials for vanadium redox flow batteries. *J. Phys. Chem. Lett.* **2012**, *3*, 2164–2167. [CrossRef]
39. Chang, Y.; Deng, L.; Meng, X.; Zhang, W.; Wang, C.; Wang, Y.; Zhao, S.; Lin, L.; Crittenden, J.C. Closed-loop electrochemical recycling of spent copper (II) from etchant wastewater using a carbon nanotube modified graphite felt anode. *Environ. Sci. Technol.* **2018**, *52*, 5940–5948. [CrossRef]
40. Wang, W.H.; Wang, X.D. Investigation of Ir-modified carbon felt as the positive electrode of an all-vanadium redox flow battery. *Electrochim. Acta* **2007**, *52*, 6755–6762. [CrossRef]
41. González, Z.; Sánchez, A.; Blanco, C.; Granda, M.; Menéndez, R.; Santamaría, R. Enhanced performance of a Bi-modified graphite felt as the positive electrode of a vanadium redox flow battery. *Electrochem. Commun.* **2011**, *13*, 1379–1382. [CrossRef]
42. Solmaz, R.; Gündoğdu, A.; Döner, A.; Kardaş, G. The Ni-deposited carbon felt as substrate for preparation of Pt-modified electrocatalysts: Application for alkaline water electrolysis. *Int. J. Hydrogen Energy* **2012**, *37*, 8917–8922. [CrossRef]
43. Wei, L.; Zhao, T.S.; Zeng, L.; Zhou, X.L.; Zeng, Y.K. Copper nanoparticle-deposited graphite felt electrodes for all vanadium redox flow batteries. *Appl. Energy* **2016**, *180*, 386–391. [CrossRef]
44. Shen, Y.; Xu, H.; Xu, P.; Wu, X.; Dong, Y.; Lu, L. Electrochemical catalytic activity of tungsten trioxide-modified graphite felt toward VO_2^+/VO^{2+} redox reaction. *Electrochim. Acta* **2014**, *132*, 37–41. [CrossRef]
45. Xiang, Y.; Daoud, W.A. Investigation of an advanced catalytic effect of cobalt oxide modification on graphite felt as the positive electrode of the vanadium redox flow battery. *J. Power Sources* **2019**, *415*, 175–183. [CrossRef]
46. Vázquez-Galván, J.; Flox, C.; Fábega, C.; Ventosa, E.; Parra, A.; Andreu, T.; Morate, J.R. Hydrogen-treated rutile TiO_2 shell in graphite-core structure as a negative electrode for high-performance vanadium redox flow batteries. *ChemSusChem* **2017**, *10*, 2089–2098. [CrossRef]
47. Bayeh, A.W.; Kabtamu, D.M.; Chang, Y.C.; Chen, G.C.; Chen, H.Y.; Liu, T.R.; Wondimu, T.H.; Wang, K.C.; Wang, C.H. Hydrogen-treated defect-rich $W_{18}O_{49}$ nanowire-modified graphite felt as high-performance electrode for vanadium redox flow battery. *ACS Appl. Energy Mater.* **2019**, *2*, 2541–2551. [CrossRef]
48. Leskelä, M.; Ritala, M. Atomic layer deposition (ALD): From precursors to thin film structures. *Thin Solid Film.* **2002**, *409*, 138–146. [CrossRef]
49. Kim, H.; Lee, H.B.R.; Maeng, W.J. Applications of atomic layer deposition to nanofabrication and emerging nanodevices. *Thin Solid Film.* **2009**, *517*, 2563–2580. [CrossRef]
50. George, S.M. Atomic layer deposition: An overview. *Chem. Rev.* **2010**, *110*, 111–131. [CrossRef]
51. Moya, A.; Kemnade, N.; Osorio, M.R.; Cherevan, A.; Granados, D.; Eder, D.; Vilatela, J.J. Large area photoelectrodes based on hybrids of CNT fibres and ALD-grown TiO_2. *J. Mater. Chem. A* **2017**, *5*, 24695–24706. [CrossRef]
52. Li, M.; Zu, M.; Yu, J.; Cheng, H.; Li, Q.; Li, B. Controllable synthesis of core-sheath structured aligned carbon nanotube/titanium dioxide hybrid fibers by atomic layer deposition. *Carbon* **2017**, *123*, 151–157. [CrossRef]
53. Geppert, T.N.; Bosund, M.; Putkonen, M.; Stühmeier, B.M.; Pasanen, A.T.; Heikkilä, P.; Gasteiger, H.A.; El-Sayed, H.A. HOR activity of Pt-TiO_{2-Y} at unconventionally high potentials explained: The influence of SIMI on the electrochemical behavior of Pt. *J. Electrochem. Soc.* **2020**, *167*, 084517. [CrossRef]
54. Lee, W.J.; Hon, M.H. Space-limited crystal growth mechanism of TiO_2 films by atomic layer deposition. *J. Phys. Chem. C* **2010**, *114*, 6917–6921. [CrossRef]
55. Lee, W.J.; Hon, M.H.; Chung, Y.W.; Lee, J.H. A three-dimensional nanostructure consisting of hollow TiO_2 spheres fabricated by atomic layer deposition. *Jpn. J. Appl. Phys.* **2011**, *50*, 06GH06. [CrossRef]

56. Lee, W.J.; Hon, M.H. An ultraviolet photo-detector based on TiO_2/water solid-liquid heterojunction. *Appl. Phys. Lett.* **2011**, *99*, 251102. [CrossRef]
57. Reich, S.; Thomsen, C. Raman spectroscopy of graphite. *Phil. Trans. R. Soc. Lond. A* **2004**, *362*, 2271–2288. [CrossRef]
58. Ferrari, A.C. Raman spectroscopy of graphene and graphite: Disorder, electron-phonon coupling, doping and nonadiabatic effects. *Solid State Commun.* **2007**, *143*, 47–57. [CrossRef]
59. Ohsaka, T.; Izumi, F.; Fujiki, Y. Raman spectrum of anatase, TiO_2. *J. Raman Spectrosc.* **1978**, *7*, 321–324. [CrossRef]
60. Tian, F.; Zhang, Y.; Zhang, J.; Pan, C. Raman spectroscopy: A new approach to measure the percentage of anatase TiO_2 exposed (001) facets. *J. Phys. Chem. C* **2012**, *116*, 7515–7519. [CrossRef]
61. Toro, R.G.; Diab, M.; de Caro, T.; Al-Shemy, M.; Adel, A.; Caschera, D. Study of the effect of titanium dioxide hydrosol on the photocatalytic and mechanical properties of paper sheets. *Materials* **2020**, *13*, 1326. [CrossRef] [PubMed]
62. Park, H.; Goto, T.; Cho, S.; Lee, S.W.; Kakihana, M.; Sekino, T. Effects of annealing temperature on the crystal structure, morphology, and optical properties of peroxo-titanate nanotubes prepared by peroxo-titanium complex ion. *Nanomaterials* **2020**, *10*, 1331. [CrossRef] [PubMed]
63. Rani, J.R.; Thangavel, R.; Oh, S.I.; Woo, J.M.; Das, N.C.; Kim, S.Y.; Lee, Y.S.; Jang, J.H. High volumetric energy density hybrid supercapacitors based on reduced graphene oxide scrolls. *ACS Appl. Mater. Interfaces* **2017**, *9*, 22398–22407. [CrossRef] [PubMed]
64. Massaglia, G.; Fiorello, I.; Sacco, A.; Margaria, V.; Pirri, C.F.; Quaglio, M. Biohybrid cathode in single chamber microbial fuel cell. *Nanomaterials* **2019**, *9*, 36. [CrossRef]
65. Abe, Y.; Hori, N.; Kumagai, S. Electrochemical impedance spectroscopy on the performance degradation of $LiFePO_4$/graphite lithium-ion battery due to charge-discharge cycling under different C-rates. *Energies* **2019**, *12*, 4507. [CrossRef]